

Mössbauer Effect in a Cubic Antiferromagnet near the Néel Point

G. K. WERTHEIM, H. J. GUGGENHEIM, H. J. WILLIAMS, AND D. N. E. BUCHANAN

Bell Telephone Laboratories, Murray Hill, New Jersey

(Received 6 February 1967)

Combined Mössbauer and magnetization measurements show that RbFeF_3 orders antiferromagnetically at $\sim 102^\circ\text{K}$ and undergoes a transition to a state with a net magnetization at 87°K . In the antiferromagnetic region both the quadrupole coupling and hyperfine effective field can be described as arising from the exchange splitting of the low-lying spin-orbit triplet. The temperature dependence of the sublattice magnetization is in accord with a critical exponent $\beta \sim \frac{1}{3}$.

INTRODUCTION

THE current interest in critical phenomena¹ prompted an examination of the Fe^{57} hyperfine structure in RbFeF_3 using the Mössbauer effect. The preparation of this cubic perovskite compound and some of its magnetic properties were reported only recently.^{2,3} This paper is concerned chiefly with the antiferromagnetic region just below the Néel point T_N . Some properties of the magnetic regions will be discussed briefly. Another interesting feature is the opportunity to determine the electric field gradient arising in a cubic material from the exchange splitting of the ground electronic state resulting from the cubic crystal field and spin-orbit coupling.

EXPERIMENTAL

The RbFeF_3 was prepared from FeF_2 made by heating high-purity metallic iron in HF at about 900°C , and from high-purity commercial RbF. Spectroscopic analyses of a number of samples are given in Table I. The major impurity K comes from the RbF and should not have significant effect on the magnetic properties. The effects of transition-metal impurities will be discussed below.

The samples used in the Mössbauer-effect studies were in the form of fine powders. Susceptibilities were measured on single crystals, free to align themselves in an easy direction. The Mössbauer spectrometer has been previously described.⁴ The source was Co^{57} in palladium.

RESULTS AND DISCUSSION

Magnetization data at 14 240 Oe (Fig. 1) show two magnetic transitions, one at 45°K and a second in the vicinity of 95°K . The spontaneous magnetization at 1.46°K was found to be $0.515\mu_B$. Above $\sim 100^\circ\text{K}$ the sample is paramagnetic.

A conventional Curie-Weiss analysis of the data in paramagnetic region yields an effective moment $\hat{p}_{\text{eff}} = 5.82\mu_B$ and a characteristic temperature $\theta = 200^\circ\text{K}$. The

susceptibility in this region can also be computed from the known energy levels and g factors of Fe^{2+} in a cubic crystal field,⁵ yielding

$$\chi = N\mu_B^2 \langle p^2(T) \rangle_{\text{av}} / 3kT, \quad (1)$$

where $\langle p^2(T) \rangle_{\text{av}}$ is a thermal average over the squares of the g factors of the 15 levels of the orbital triplet (Fig. 2). Unfortunately, the effect of exchange cannot be rigorously introduced into this expression by replacing T by $T + \theta$.

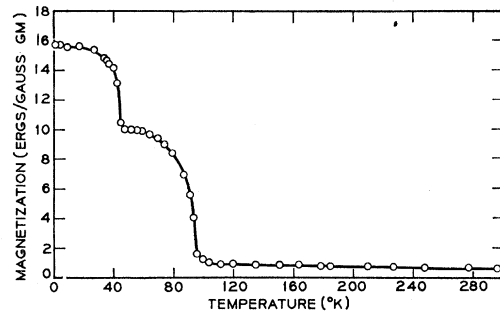


FIG. 1. Magnetization of RbFeF_3 at 14 240 Oe.

We have nevertheless attempted to analyze the data in terms of the resulting expression, first computing $\langle p^2(T) \rangle_{\text{av}}$ for $\lambda = -100 \text{ cm}^{-1}$ and $\lambda/Dq = 0.1$. (The calculations are not very sensitive to the choice of λ/Dq .) Satisfactory agreement between theory and experiment is obtained for $\theta = 130^\circ\text{K}$, provided there is also a sizeable temperature-independent paramagnetism, $\chi_0 \sim 20 \times 10^{-6} \text{ erg/G g}$. Note, however, that the data at hand do not extend over a sufficient range of temperature to make it possible to determine λ , Dq , θ , and χ_0 independently. As a result of this and of the difficulty encountered in introducing exchange, this approach is of doubtful value in the present case.

The transition at 95°K was examined in greater detail as a function of magnetic field using a Foner vibrating sample magnetometer. Data taken in external fields as low as 500 Oe show a dependence on temperature and magnetic field quite different from that expected for a second-order phase transition between a paramagnetic and a ferromagnetic state. This is in accord with the Mössbauer measurements discussed below which show that the region above the transition is

¹ See, for example, Proceedings of the Conference on Critical Phenomena, Washington, D.C., 1965, edited by Green and Sengers, Natl. Bur. Std. (U.S.) Misc. Publ. 273, 3f (1966).

² M. Kestigian *et al.*, Inorg. Chem. 5, 1462 (1966).

³ F. F. Y. Wang and M. Kestigian, J. Appl. Phys. 37, 975 (1966).

⁴ G. K. Wertheim, *Mössbauer Effect, Principles and Applications* (Academic Press Inc., New York, 1964), Chap. II.

⁵ W. Low and M. Weger, Phys. Rev. 118, 1119 (1960).

antiferromagnetically ordered. A transition temperature of 87°K was obtained using a linear extrapolation to zero field.

Mössbauer absorption spectra taken in the vicinity of the 87°K transition are shown in Fig. 3. The data at 82.0°K, which are characteristic of the magnetic region from 45 to 87°K, show a superposition of hyperfine structures due to two magnetically inequivalent iron sites. The data at 94.3°K, characteristic of the region from 87 to 102°K, show the hyperfine structure of single iron site with both magnetic and quadrupolar coupling. The data at 127°K are characteristic of the paramagnetic region in which the absorption is unsplit.

The absence of remanence in the magnetization measurements together with the Mössbauer-effect re-

TABLE I. Spectroscopic analysis of samples used in this investigation. The impurity concentrations are in percent, X denotes "any digit," NF means "none found."

	Sample number			
	853	664	1235	1050
Ni	0.0X low	NF	0.0X	0.0X
Si	0.0X low	0.00X	0.00X	0.000X
Mn	0.00X low	0.0X	0.000X	0.00X
Mg	0.000X low	0.000X	0.000X	0.000X
Al	0.00X low	0.00X	0.00X	NF
Cu	0.00X	0.00X	0.00X	NF
Pb	0.00X	0.00X	NF	NF
Ag	0.000X	NF	NF	NF
Co	NF	NF	NF	NF
K	0. X	0. X	0. X	0. X
Ca	0.00X	0.00X	0.00X	0.00X
Na	0.00X	0.00X low	0.00X low	0.000X
Cs	0.00X	0.00X	0.00X low	NF

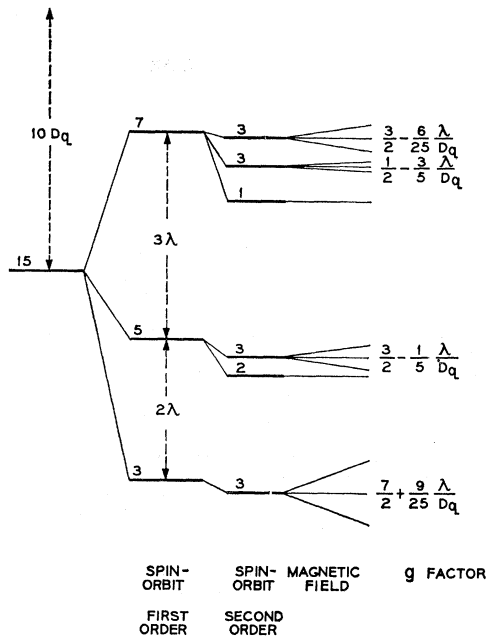


FIG. 2. Energy-level scheme of the orbital triplet in weak magnetic field, according to Low and Weger (Ref. 5).

sults clearly show that antiferromagnetic (AFM) order exists above 87°K. This region was then re-examined with greater sensitivity in an attempt to observe a discontinuity in the slope of the susceptibility at the Néel point. None was detected. The reason for this failure subsequently became apparent when this AFM transition was found to be spread over a few degrees Kelvin (see below).

The behavior of RbFeF_3 in the vicinity of 87°K is reminiscent of that⁶ of KMnF_3 which orders antiferromagnetically at 88.3°K and cants at 81.5°K. The 87°K transition in RbFeF_3 is not describable as a canting, however, since the Mössbauer spectra below the transition show a superposition of two quite different hyperfine structures, suggesting ferrimagnetic order. This

⁶ A. J. Heeger, Olof Beckman, and A. M. Portis, Phys. Rev. **123**, 1652 (1961).

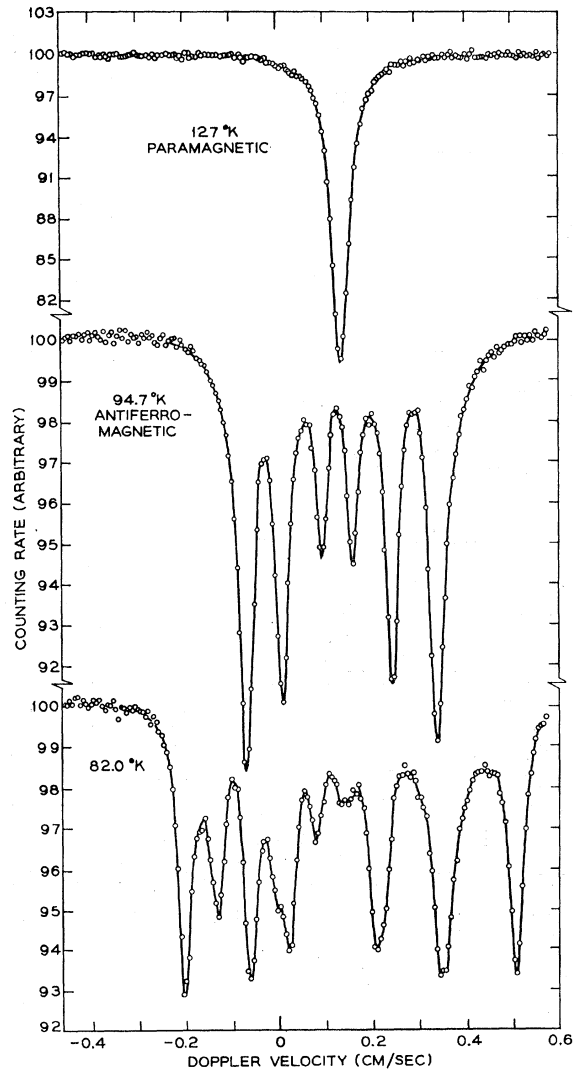


FIG. 3. Examples of Mössbauer spectra in the paramagnetic, antiferromagnetic, and ferrimagnetic regions.

TABLE II. Summary of data. The first set was taken with sample 1050, the second with one containing 0.X Ni, Mn, and Cu.

Temperature °K	H_{eff} kOe	Quadrupole splitting cm/sec	$\Delta E_Q/H_{\text{eff}}^2$ cm/sec kOe ²	Remarks
82.0	12 lines
84.2	12 lines
86.0	12 lines
88.2	153.0	0.0147	0.63×10^{-6}	6 lines
90.3	143.3	0.0125	0.61	6 lines
91.6	139.5	0.0110	0.57	6 lines
92.6	134.2	0.0105	0.58	6 lines
94.3	126.8	0.0092	0.57	6 lines
96.3	113.1	0.0064	0.50	6 lines
98.4	94.2	~ 0.006	~ 0.68	6 lines
100.0	~ 82.5	6 lines
102.1	Broadened
127	0	0	...	single line
82.5	Mixed spectrum
83.6	166.0	0.019	0.69	6 lines
86.0	158.0	0.0161	0.65	6 lines
87.9	152.0	0.0149	0.64	6 lines
90.4	144.0	0.0132	0.64	6 lines
92.6	133.7	0.0109	0.61	6 lines
94.8	122.0	0.0087	0.58	6 lines
96.8	109.2	0.0075	0.63	6 lines
98.2	99.5	0.0055	0.56	6 lines
99.0	89.1	6 lines
100.2	78.7	6 lines
101.3	Broadened
102.3	0	0	...	single line

will not be explored further in this paper. The Mössbauer-effect measurements also provide a direct zero-field determination of the location of the 87°K transition, and confirm that it is depressed by transition-metal impurities. Results obtained for two samples of widely differing impurity content agree within the error of measurement in the antiferromagnetic region. From this point on we confine ourselves to a detailed examination of the magnetic hyperfine and electric quadrupole splitting in the antiferromagnetic region (Table II).

ORIGIN OF THE ELECTRIC FIELD GRADIENT

The electric field gradient (EFG) could arise from a lattice distortion accompanying the AFM transition or from the splitting of the low-lying spin-orbit triplet by the exchange field. An x-ray determination⁷ has not shown any measurable distortion from the cubic perovskite structure in the antiferromagnetic region, making it unlikely that this mechanism is responsible for EFG. The other mechanism predicts both the magnitude of the quadrupole splitting and its temperature dependence and therefore allows a critical test.

The energies of the lowest states of Fe²⁺ in a pure cubic crystal field including the effects of spin-orbit coupling and the action of a weak magnetic field are⁷

$$E_0 = 4Dq + 3\lambda + \frac{9}{25}(\lambda^2/Dq),$$

$$E_{\pm 1} = 4Dq + 3\lambda + \frac{9}{25}(\lambda^2/Dq) \pm \left[\frac{7}{2} + \frac{9}{25}(\lambda/Dq) \right] \beta H. \quad (2)$$

The next higher lying states are separated by 2λ ($\lambda \sim -100$ cm⁻¹) from the ground triplet and will

⁷ H. J. Levinstein (private communication).

therefore be neglected below 100°K.^{7a} A perturbation theory treatment which avoids this approximation, but leads to qualitatively similar conclusions has been obtained by Ganiel.^{7a}

By using the t_{2g} - p equivalence the corresponding wave function may be reduced to the form

$$\begin{aligned} |\Gamma_5 0\rangle &= (3/10)^{1/2} | -11 \rangle + (3/10)^{1/2} | 1-1 \rangle \\ &\quad - (4/10)^{1/2} | 10 \rangle, \\ |\Gamma_5 \pm 1\rangle &= - (3/10)^{1/2} | \pm 10 \rangle \\ &\quad + (6/10)^{1/2} | \pm 2 \mp 1 \rangle + (1/10)^{1/2} | 0 \pm 1 \rangle. \quad (3) \end{aligned}$$

The EFG produced by these states is obtained using the well-known result⁸ that the EFG due to $|xz\rangle$ and $|yz\rangle$ is $-(2/7)e\langle r^{-3} \rangle$ while that due to $|xy\rangle$ is $(4/7)e\langle r^{-3} \rangle$, yielding

$$\begin{aligned} \langle V_{zz} \rangle_0 &= \frac{1}{10} [(4/7)e\langle r^{-3} \rangle], \\ \langle V_{zz} \rangle_{\pm 1} &= -(1/20) [(4/7)e\langle r^{-3} \rangle]. \quad (4) \end{aligned}$$

The EFG resulting from this triplet at temperature T and external field H is then readily shown to be

$$\langle V_{zz} \rangle = \frac{-1}{20} \left[\frac{4}{7} e \langle r^{-3} \rangle \right] \frac{\cosh w - 1}{\cosh w + \frac{1}{2}}, \quad (5)$$

where

$$w = g\beta H/kT,$$

and

$$g = \frac{7}{2} + \frac{9}{25}(\lambda/Dq).$$

The largest quadrupole splitting found in the AFM region (0.019 cm/sec) approaches the saturation value

^{7a} U. Ganiel (private communication).

⁸ R. Ingalls, Phys. Rev. **133**, A787 (1964).

of 0.0225 cm/sec obtained from the above equations using the numerical values for the quadrupole moment and shielding factor given by Ingalls³ with the reduction factor $F=1/20$.

The expression for the quadrupole splitting ΔE_Q at temperature T and external field H is

$$\Delta E_Q = -0.0225(\cosh w - 1)/(\cosh w + \frac{1}{2}) \quad (6)$$

The measured sign of the quadrupole splitting indicates that the spin align in a (111) direction rather than the (100) direction assumed in the treatment of Ref. 5 and in the above.^{7a}

ESTIMATE OF HYPERFINE EFFECTIVE FIELD

The effective field H_{eff} at the nucleus due to the triplet state may be similarly evaluated. From Eq. (2) the expectation values of spin and orbital angular momentum for $g\beta H/kT \gg 1$ are $\langle S_z \rangle = \frac{3}{2}$ and $\langle L_z \rangle = -\frac{1}{2}$. The core polarization contribution to H_{eff} in Fe^{2+} for $S_z=2$ has been estimated to be -550 kOe,⁹ yielding in the present case -412 kOe. The orbital contribution H_{orb} is

$$H_{\text{orb}} = -2\mu_B \langle r^{-3} \rangle \langle L_z \rangle. \quad (7)$$

Using $\langle r^{-3} \rangle = 4.8$ atomic units (a.u.) and an orbital reduction factor of 0.8 we obtain $H_{\text{orb}} = 240$ kOe. The dipolar contribution is estimated to be less than 5 kOe and will be neglected. The expected value for H_{eff} is then 172 kOe at saturation,¹⁰ and the effective field at temperature T and external field H is given by

$$H_{\text{eff}} = 172 \frac{\sinh w}{\cosh w + \frac{1}{2}}. \quad (8)$$

We will now assume that the effect of exchange in the AFM region may be represented by a magnetic field H_{ex} . Equation (5) and (8) then give a relationship between quadrupole splitting and hyperfine field through the exchange field as a parameter. To facilitate comparison between theory and experiment, the dependence on the exchange field may be largely eliminated by computing $\Delta E_Q/H_{\text{eff}}^2$. In the limit of $g\beta H/kT \ll 1$ this ratio is 0.56×10^{-6} cm/sec (kOe)², while for $g\beta H/kT \gg 1$ it is 0.76×10^{-6} . It changes monotonically between these two limits. The experimental values range from $(0.5 \pm 0.1) \times 10^{-6}$ to $(0.7 \pm 0.1) \times 10^{-6}$. The large uncertainties arise from the quadrupole splitting which is never greater than the theoretical linewidth. One should not attach much significance to the numerical agreement since the evaluation of H_{eff} allows considerable latitude. More important is the fact that the experimental ratio of $\Delta E_Q/H_{\text{eff}}^2$ varies only slowly with temperature as predicted by the theory, confirming that the origin of the electric field gradient lies in the exchange splitting of the ground state.

⁹ A. J. Freeman and R. E. Watson, in *Magnetism*, edited by G. T. Rado and H. Suhl (Academic Press Inc., New York, 1965), Vol. IIA, p. 167.

¹⁰ The field in KFeF_3 has been estimated to be -140 kOe [Okiji and Kanamori, J. Phys. Soc. Japan **19**, 908 (1964)].

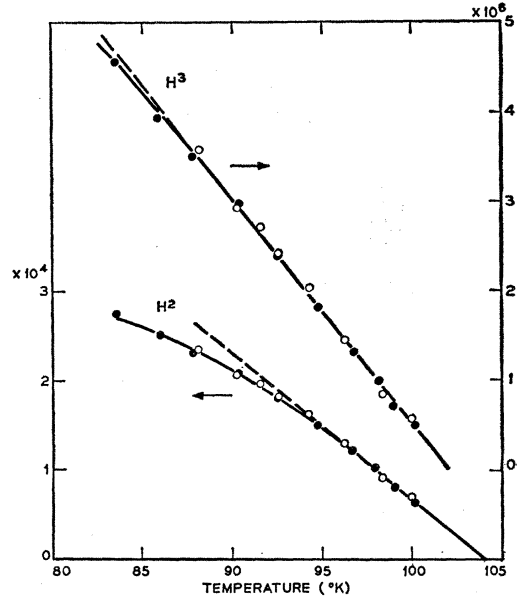


FIG. 4. Determination of the Néel temperature and of the critical exponent β . Data from two samples differing in purity are shown.

MAGNETIZATION NEAR CRITICAL POINT

The temperature dependence of the sublattice magnetization near a critical point may be represented by an equation of the form¹

$$M(T) \propto (1 - T/T_N)^\beta. \quad (9)$$

The molecular-field model predicts $\beta = \frac{1}{2}$. The three-dimensional Ising-model theories predict $\beta = \frac{1}{3}$.¹¹ We test these two exponents by plotting H^2 and H^3 against temperature (Fig. 4) assuming that H_{eff} is proportional to the sublattice magnetization. It is apparent that the latter gives a fit to the data over a wider range of temperature, but it is not *a priori* clear how far from the Néel temperature this representation should be valid. In the case of MnF_2 ,¹² a good fit was obtained in the range $0.0001 < (1 - T/T_N) < 0.1$ for $\beta = 0.333$. In the present case the data cover the range $0.02 < (1 - T/T_N) < 0.15$ and are well represented by $\beta = \frac{1}{3}$ up to ~ 0.1 . The disagreement above 0.1 is not surprising since a magnetic phase change takes place at 0.15. The fit for $\beta = \frac{1}{2}$ is much more restricted in temperature. The use of $\beta = \frac{1}{3}$ gives a Néel temperature of 102.0°K.

A more detailed analysis of the critical behavior is precluded by line broadening which becomes severe as much as 2°K below the Néel point. As the Néel point is approached from below, severe line broadening characteristic of a spread in hyperfine fields is observed. It is orders of magnitude greater than can be accounted for by the temperature fluctuations in the absorber. At and above the Néel temperature the spectrum

¹¹ E. Callen and H. Callen, J. Appl. Phys. **36**, 1140 (1965).

¹² P. Heller, Phys. Rev. **146**, 403 (1966).

consists of an unsplit component and an unresolved broad absorption whose width indicates that it is of magnetic origin. The width is too great to be of quadrupolar origin resulting from slow relaxation.¹³ Experiments with crystals of widely differing impurity contents prove that this effect is not due to transition-metal impurities. The effect extends over much too great a temperature range to be related to critical-point fluctuations. The most probable explanation lies in lattice strain sufficient to perturb the threefold de-

¹³ F. S. Ham (to be published).

generate ground states by an amount sufficiently large to cause a spatial variation of the Néel temperature.

ACKNOWLEDGMENTS

The authors are indebted to H. J. Levinstein for permission to quote his x-ray results prior to publication, to M. D. Sturge and L. R. Walker for valuable discussions, to J. L. Davis for the low-field susceptibility measurements, and to F. F. Wang and M. Kestigian for a sample of RbFeF₃, which gave results in good agreement with our own.

Magnetic Structures of Holmium. II. The Magnetization Process*

W. C. KOEHLER, J. W. CABLE, H. R. CHILD, M. K. WILKINSON, AND E. O. WOLLAN

Solid State Division, Oak Ridge National Laboratory, Oak Ridge, Tennessee

(Received 9 January 1967)

Neutron-diffraction measurements have been made on single-crystal holmium at temperatures ranging from 4.2 to 120°K in applied magnetic fields up to 22.3 kOe in order to study the magnetization process of this material. At low temperatures, the *b* direction in the basal plane is an easy axis. For a field applied parallel to an *a* direction, the moments are aligned parallel to the closest *b* directions. At higher temperatures the effect of a field applied parallel to a *b* direction is to transform the system to a *b*-axis ferromagnet after causing it to pass through one or two (depending upon the temperature) intermediate fanlike oscillatory structures. Similar oscillatory configurations are produced by the application of a field parallel to an *a* direction. The *a*-axis ferromagnet is not produced in fields up to 22.3 kOe. A characterization of the four intermediate structures observed at 50°K was made and schematic phase diagrams in the *H-T* plane were extracted from the diffraction and magnetization data. Studies of the remanent state at 4.2°K were made, and are reported.

INTRODUCTION

IN an earlier paper¹ we have described the virgin-state magnetic structures of holmium as deduced from single-crystal neutron-diffraction experiments. From the Néel temperature to about 20°K, the moments order in a helical structure in which the *c* axis is the screw axis. Below 20°K the structure is a ferromagnetic spiral in which a net moment of $1.7\mu_B$ is found along the *c* axis. At low temperatures the configuration in the basal plane is a distorted helical one in which moments of magnitude $9.5\mu_B$ are bunched around the *b* directions. The work was based on studies of two crystals: Ho(*A*), with a final turn angle of 36.7° per layer, and Ho(*B*), with a final turn angle at 4.2°K of precisely 30.0° per layer. As described earlier, the latter crystal appears to be more nearly representative of pure, strain-free, holmium.

In this paper we report results of neutron-diffraction studies which have been made on these crystals in applied magnetic fields. Most of the work reported deals with the crystal (*B*) for which accurate demagnetization corrections could be made. A few results, particularly those obtained at low temperature, are given for Ho(*A*).

These experiments were undertaken to understand

the apparent discrepancy between the early magnetization data,² which indicated a transition to a completely ferromagnetic state, and the virgin-state diffraction results, and to investigate the origin of the many anomalies in the single-crystal magnetization curves reported by Strandburg, Legvold, and Spedding.³ It seems particularly appropriate now to characterize as well as possible the magnetic structures induced by the application of a steady magnetic field because the knowledge of such structures will be important to the interpretation of experiments, such as magnetic resonance and inelastic neutron scattering, designed to investigate spin-wave excitations in the rare earths.

Theoretical studies of the magnetization process of a helical spin structure were made first by Herpin and Mériel,⁴ and by Enz.⁵ The most complete investigations have been made by Nagamiya and his associates⁶ who studied the changes in helical and other oscillatory spin structures due to the application of a magnetic field at finite temperatures, as well as at absolute zero, and for a number of cases of different anisotropy energy.

² B. L. Rhodes, S. Legvold, and F. H. Spedding, *Phys. Rev.* **109**, 1544 (1958).

³ D. L. Strandburg, S. Legvold, and F. H. Spedding, *Phys. Rev.* **27**, 2046 (1962).

⁴ A. Herpin and P. Mériel, *Compt. Rend.* **250**, 1450 (1960); *J. Phys. Radium* **22**, 337 (1961).

⁵ U. Enz, *Physica* **26**, 69 (1960); *J. Appl. Phys.* **32**, 22S (1961).

⁶ T. Nagamiya, K. Nagata, and Y. Kitano, *Progr. Theoret. Phys. (Kyoto)* **27**, 1253 (1962); Y. Kitano and T. Nagamiya, *ibid.* **31**, 1 (1964).

* Research sponsored by the U.S. Atomic Energy Commission under contract with the Union Carbide Corporation.

¹ W. C. Koehler, J. W. Cable, M. K. Wilkinson, and E. O. Wollan, *Phys. Rev.* **151**, 414 (1966).